Anti-SARS and anti-HCV drugs repurposing against the Papain-like protease of the newly emerged coronavirus (2019-nCoV)

Abdo Elfiky (abdo@sci.cu.edu.eg)
Cairo University https://orcid.org/0000-0003-4600-6240
Noha S Ibrahim
Cairo University

Research Article

Keywords: Wuhan coronavirus, 2019-nCoV PLpro, docking, Grazoprevir, Telaprevir, drug repurposing

Posted Date: February 11th, 2020

DOI: https://doi.org/10.21203/rs.2.23280/v1

Abstract

A new mysterious coronavirus outbreak started last month in China. The World Health Organization (WHO) termed the new virus strain 2019-nCoV to be the seventh reported human coronaviruses (HCoV). A seafood market in Wuhan city, central China was the starting point of the emergence with unknown animal causes the first animal to human infection. Until today 904 confirmed deaths and more than 40000 cases confirmed in China and 28 countries. There is a massive fear of the human to human transmission of 2019-nCoV that reported last week by the Chinese government. The most famous two strains of HCoV are the Severe Acute Respiratory Syndrome coronavirus (SARS CoV) and the Middle East Respiratory Syndrome coronavirus (MERS CoV). The former had emerged in China in 2002 while the latter emerged in the Middle East region in 2012 and south Korea in 2015. In this study, the newly emerged 2019-nCoV papain-like protease (PL^{pro}) is targeted by anti-SARS PL^{pro} drugs and the anti-Hepatitis C Virus (HCV) Non-structural protein 3 (NS3) serine protease drugs. Sequence analysis, modeling, and docking are used to get a valid model for 2019-nCoV PL^{pro}. The results suggest the effectiveness of the anti-SARS drugs (GRL-0667, GRL-0617, and Mycophenolic acid) and the anti-HCV drugs (Grazoprevir, Telaprevir, and Boceprevir) as potent inhibitors against the newly emerged coronavirus.

Introduction

A New emerged human coronavirus (2019-nCoV) is reported last month in Wuhan city in China [1,2]. According to the World Health Organization (WHO) surveillance draft two weeks ago, any traveler to Wuhan, Hubei Province in China, 15 days before the onset of the symptoms, is suspected to be a 2019-nCoV patient [2,3]. Additionally, WHO distributed interim guidance for laboratories that carry out the tests for the emerged outbreak and it releases infection prevention and control guidance [4,5]. 2019-nCoV viral pneumonia is related to the seafood market when an unknown animal is responsible for the emergence of the outbreak [1]. Other countries started their surveillance borders to prevent the spread of the new unknown coronavirus especially when the Chinese new year holiday is in effect [6]. Until 20 days ago, 41 cases are confirmed to be 2019-nCoV positives leaving one dead and seven in critical care. This number is grossly increasing every day and the number of confirmed cases at the date of writing this manuscript is more than 1400 and 80 deaths are confirmed in China (50 infections confirmed outside China) [7]. The National Health Commission of China confirmed the human-to-human transmission of the Wuhan outbreak (2019-nCoV) five days ago [7]. The symptoms include fever, malaise, dry cough, shortness of breath, and respiratory distress [1].

2019-nCoV is a member of *Betacoronaviruses* family such as the Severe Acute Respiratory Syndrome Human coronavirus (SARS HCoV (8000 infections from which 774 dead)) and the Middle-East Respiratory Syndrome Human coronavirus (MERS HCoV (2500 infections from which 858 dead)) [8,9]. All the human coronaviruses (HCoVs) are zoonotic viruses that transmit from animals to humans through

direct contact. Until today, seven different strains of Human coronaviruses (HCoVs) have been reported, including the newly emerged 2019-nCoV [1,10]. 229E and NL63 strains of HCoVs belong to *Alphacoronaviruses* while OC43, HKU1, SARS, MERS, and 2019-nCoV HCoVs belong to *Betacoronaviruses* [1,8]. SARS and MERS HCoV are the most aggressive strains of coronaviruses, leaving about 800 deaths each. SARS HCoV has a 10% mortality rate, while MERS HCoV has a 36% mortality rate, according to the WHO [8,10-13]. For the newly emerged coronavirus, the mortality rate is far lower (3%) than that of SARS and MERS but the fear is from its high transmission rate (human to human).

HCoVs generally are positive-sense single-stranded RNA (30kb) viruses. Two groups of protein characterize HCoVs; structural, such as Spike (S), Nucleocapsid (N) Matrix (M) and Envelope (E), and non-structural proteins such as RNA dependent RNA polymerase (RdRp) (nsp12) and the Papain-like protease PL^{pro} [8]. PL^{pro} is an essential enzyme in the life cycle of RNA viruses, including coronaviruses. PL^{pro} is a multifunctional cysteine protease that processes the viral polyprotein and host cell proteins by hydrolysing the peptide and isopeptide bonds in viral and cellular substrates leading to the virus replication (Baez-Santos et al. 2014). PL^{pro} is targeted in different coronaviruses viruses, including SARS, MERS, and HCV [14-18].

In this study, the 2019-nCoV PL^{pro} model is generated using homology modeling after sequence comparison to the solved structures in the protein data bank [19]. Molecular docking is then performed to test some drugs (anti-SARS PL^{pro} and anti-HCV NS3) against 2019-nCoV PL^{pro}. The results suggest possible inhibition for the currently available therapeutics against the newly emerged coronavirus *in silico*.

Materials And Methods

Sequence alignment and modeling

The deposited gene for the newly emerged 2019-nCoV NC_045512.2 (last updated 17 January 2020) is retrieved from the National Center for Biotechnology Information (NCBI) nucleotide database then translated using ExPASy translate tool [20 21]. Swiss Model is used to build a model for 2019-nCoV PL^{pro} [22]. Using Basic Local Alignment Search Tool (BLAST) against the 2019-nCoV PL^{pro} we found eight different solved structures for SARS PL^{pro} (PDB IDs: 5TL6, 2FE8, 5E6J, 3MJ5, 5Y3E, 4M0W, 3E9S, and 4OVZ) that have at least 82.17% sequence identity to 2019-nCoV PL^{pro} [23]. We choose the 5Y3E, chain A, because it is the best resolution (1.6 Å) structure among the eight SARS PL^{pro}. Therefore, 5Y3E is used as a template (82.8 % identity) for building 2019-nCoV PL^{pro} using the Swiss Model. Validation of the model is assessed by the Molprobity web server (Duke University), and the structure analysis and verification server (SAVES) (University of California Los Angles) [24,25]. PROCHECK [26], Verify 3D [27], PROVE [28], and ERRAT [29] in addition to the Ramachandran plot of the Molprobity are used to judge the validity of the model. Accordingly, the model is further energy minimized (MM3 force field), after the addition of missing

Hydrogen atoms, by the computational chemistry workspace SCIGRESS to be ready for the docking experiments [14,17,30-32].

Molecular Docking

Docking experiments are performed on the optimized 2019-nCoV PL^{pro} and the SARS PL^{pro} (PDB ID: 5Y3E, chain A) by the aid of AutoDock Vina software [33]. six different compounds (three anti-SARS and three anti-HCV) are tested against 2019-nCoV PL^{pro}. The anti-SARS compounds were N-(1,3-benzodioxol-5-ylmethyl)-1-[(1R)-1-naphthalen-1-ylethyl]piperidine-4-carboxamide (GRL-0667) [34], 5-amino-2-methyl-N-[(1R)-1-naphthalen-1-ylethyl]benzamide (GRL-0617) [35], and Mycophenolic acid [36], while the anti-HCV drugs were the three approved (by FDA) drugs Telaprevir [37], Boceprevir [38], and Grazoprevir [39].

After docking, the structures are analyzed through the Protein-Ligand Interaction Profiler (PLIP) web server (Technical University of Dresden) [40].

Results And Discussion

2019-nCoV PL^{pro} *modeling*

Figure 1A shows the pairwise sequence alignment of the PL^{pro} of SARS and 2019-nCoV strains of coronavirus. SARS HCoV PL^{pro} secondary structure is presented at the top of the alignment (PDB ID: 5Y3E chain: A) while its water accessibility is presented at the bottom with blue indicating highly accessible residues, cyan partially accessible while white for the buried residues. Three black-dashed rectangles mark the active site residues (C112, H273, and D287) of both SARS HCoV and 2019-nCoV PL^{pro}. Figure 1B shows the pairwise sequence alignment of 2019-nCoV PL^{pro} versus HCV NS3 (PDB ID: 3SU6). Orange-dashed rectangles surround the active site residues of HCV NS3 (H78, D102, and S159). As implied from the alignment, SARS PL^{pro} versus 2019-nCoV PL^{pro} shows high conservation (highlighted in red), called sequelogous. Despite the pairwise percent identity of 2019-nCoV PL^{pro} against SARS HCoV PL^{pro} is 82.8%, and only 11.85% for HCV NS3, the similarity to 2019-nCoV PL^{pro} is 93.81% and 59.68% for SARS PL^{pro} and HCV NS3, respectively. The active site triad C112, H273, and D287 of both SARS HCoV and 2019-nCoV PL^{pro} (figure 1A) are partially surface accessible in order for PL^{pro} to be able to attach its substrates for cleavage [41]. For HCV NS3, the active site residues H78 and D102 are surface accessible as well (figure 1B) [42]. This can be deduced from figure 1C, where the 2019-nCoV PL^{pro} model is represented by PyMOL software in the surface (right) and carton (left) representations. The three active site residues are in red (surface accessible) while the rest of the residues in green (see the enlarged panel). The surface accessibility is vital for the function of the protease, allowing the interaction with the substrates.

Figure 1 (A) Pairwise sequence alignment of SARS HCoV PLpro (PDB ID: 5Y3E) against the Wuhan 2019-nCoV PLpro. (B) Pairwise sequence alignment of HCV NS3 (PDB ID: 3SU6) against the Wuhan 2019-nCoV

PLpro. Red highlights indicate identical residues, while yellow highlights are less conserved. Secondary structures are represented at the top of the alignments, while the surface accessibility is shown at the bottom (blue: highly accessible, cyan: partially accessible, while white is for buried). The black dashed rectangles mark active sites of both 2019-nCoV PLpro and SARS PLpro (C112, H273, and D287) while orange rectangles mark the active site of HCV NS3 (H78, D102, and S159). The alignment is performed using the CLUSTAL omega web server and represented by ESpript 3. (C) The newly emerged Wuhan 2019-nCoV PLpro model built by Swiss Model in the green cartoon (left) and surface (right) representations. The active site residues are represented in red sticks for clarification (see the enlarged panel).

The complete genome for 2019-nCoV has a BLAST sequence identity of 89.12 % and 82.34% with Bat SARS-like coronavirus isolate *bat-SL-CoVZC45* and SARS coronavirus *ZS-C*, respectively. Drug designers should take care of the identity, especially when emerging RNA viruses that have a high mutation rate are targeted. On the other hand, potent drugs could undetectably present on shelves able to stop the rapidly emerging 2019-nCoV strain.

2019-nCoV PL^{pro} model (315 residues) is built by the aid of the Swiss Model using SARS HCoV PL^{pro} (PDB ID: 5Y3E, chain A) as a homolog. The model is sequelogous (82.8% id) to the template suggesting a high-quality model obtained. The model is valid based on the values of the Ramachandran plot (100% in the allowed region and 92.9% in the most favored region). Besides, 92.04% of the residues have averaged a 3D-1D score of ≤ 0.2 (Verify 3D software), while the overall quality factor (ERRAT software) is 94.8%. PROVE software gives 2.7% atomic volumes outliers, which is acceptable.

Figure 2 2D structures of the anti-SARS PLpro drugs (top) (GRL-0667, GRL-0617, and Mycophenolic acid) and anti-HCV NS3 drugs (bottom) (Telaprevir, Boceprevir, and Grazoprevir) retrieved from PubChem database. Carbon atoms not explicitly represented by a letter, but with black lines, N stands for Nitrogen, O stands for Oxygen, S stands for Sulfur, and H stands for Hydrogen.

Anti-SARS and anti-HCV binding to 2019-nCoV PL^{pro}

Before performing the docking experiments, the structures of the small molecules, the 2019-nCoV PL^{pro} model and SARS PL^{pro} structure (PDB ID: 5Y3Q, Chain A), are prepared. The missing Hydrogen atoms are added to the protein structure and model, while any water molecules or ligands are removed from the SASR structure. Ligand structures are retrieved from the protein data bank files to be in the optimized active form. Figure 2 shows the 2D structures of the anti-SARS PL^{pro} (top) and anti-HCV NS3 (bottom) drugs. The anti-SARS PL^{pro} GRL-0667, GRL-0617, and mycophenolic acids are retrieved from the PDB files 3MJ5 (GRM), 3E9S (TTT), and 1JR1 (MOA), respectively. Besides, the anti-HCV NS3 Telaprevir, Boceprevir, and Grazoprevir are retrieved from the PDB files 3SV6 (SV6), 3LOX (MCX), and 3SUD (SUE), respectively.

The active site of the proteins (2019-nCoV PL^{pro} and SARS PL^{pro}) is treated as flexible during the docking experiments. A grid box of size 30 Å × 36 Å × 30 Å centered at (-17.9, 43.9, 1.6) Å is prepared for 2019-nCoV PL^{pro} utilizing the AutoDock tools [43]. Additionally, a grid box of size 30 Å × 34 Å × 30 Å centered at (-75.6, -3.8, 109.8) Å is prepared for SARS PL^{pro}. AutoDock Vina is used to predicting the interaction between the anti-SARS and anti-HCV proteases drugs against the active site of 2019-nCoV PL^{pro}. Figure 3 shows the docking score values for 2019-nCoV PL^{pro} (blue line), SARS HCoV PL^{pro} (orange line), and HCV NS3 (gray line).

Figure 3 Binding energies calculated by AutoDock Vina for the docking of the anti-SARS PLpro drugs (GRL-0667, GRL-0617, and Mycophenolic acid) and anti-HCV NS3 drugs (Telaprevir, Boceprevir, and Grazoprevir) against 2019-nCoV PLpro (blue line), SARS PLpro (orange line), and HCV NS3 (gray line).

As reflected from the docking scores, the six compounds can bind to 2019-nCoV PL^{pro}, SARS HCoV PL^{pro}, and HCV NS3 with good binding energy (-5.7 up to -11.0 kcal/mol). There is a reduction in the binding energies for the drugs to 2019-nCoV PL^{pro} compared to other proteases. For GRL-0667, GRL-0617, and Mycophenolic acid, the reduction in the binding energies for 2019-nCoV PL^{pro} is 25%, 21%, and 30%, respectively compared to SARS PL^{pro}. While, in the case of HCV, the reduction in the 2019-nCoV PL^{pro} binding energies is 18%, 11%, and 38% for Telaprevir, Boceprevir, and Grazoprevir, respectively. Despite this reduction, the PL^{pro} of 2019-nCoV still able to bind the drugs with good binding energies (-5.7 up to -7 kcal/mol), which is enough to maintain the viral protein dysfunctionally.

To further analyze the binding patterns, we examined the interaction complexes formed upon docking by the aid of the PLIP web server. Figures 4A and 4B show the interactions that formed after docking of the anti-SARS (GRL-0667, GRL-0617, and Mycophenolic acid) and anti-HCV drugs (Telaprevir, Boceprevir, and Grazoprevir), respectively. The solid blue lines indicate H-bonding, while dashed grey lines indicate hydrophobic interactions. The salt bridges and the π-π contacts are represented in balls connected by yellow dashed lines, and green dashed lines, respectively. The labeled residues (blue sticks) represent the 2019-nCoV active residues that interact with the ligands (orange sticks). Tables 1 and 2 show the interaction pattern that established upon docking for the anti-SARS drugs and the anti-HCV drugs, respectively. The binding energies are listed in the table along with the number of formed H-bonds and the number of hydrophobic interactions established after docking. The amino acids from the 2019-nCoV PL^{pro} that engaged in the interaction with the ligands are listed as well in tables 1 and 2.

Figure 4 The interaction pattern for 2019-nCoV PLpro against the anti-SARS PLpro (A) and anti-HCV NS3 (B). PyMOL software is used to represent the docking poses using colored sticks. Orange sticks represent the drugs while blue stick for the 2019-nCoV PLpro residues involved in the binding (labeled with its three-letter codes). Blue solid lines represent H-bonds while hydrophobic interactions are grey-dashed lines. Salt

bridges and π-π contacts are in dashed lines between two yellow spheres and green-dashed lines, respectively.

Additionally, the results of the interactions of SARS PL^{pro} against anti-SARS drugs are listed in table 1, while the anti-HCV drugs' interactions with HCV NS3 are listed in table 2 for comparison. The most-reported residues from the 2019-nCoV PL^{pro} that take part in the interaction through H-bonding or hydrophobic interactions are K105 and W106 (bold residues in tables 1 and 2). As implies from the tables, both SARS PL^{pro} and HCV NS3 have a higher number of interactions established upon docking the tested drugs compared to the new coronavirus strain. However, there are a minimum number of established interactions (seven interactions) that stabilize the drugs in the protein active site for 2019-nCoV PL^{pro}. Besides, in all docking experiments, the established interactions are both H-bonding and hydrophobic interactions in addition to few salt bridges (stared residues in the tables 1 and 2) suggesting the possibility of these drugs (anti-SARS and anti-HCV drugs) to bind to and inhibit the function of the crucial viral enzyme PL^{pro}.

Table 1 The interactions formed between anti-SARS compounds (GRL-0667, GRL-0617, and Mycophenolic acid) and 2019-nCoV PL^{pro} upon docking. The Star (*) represents salt bridges while the douple stars (**) represents π-π contact.

Anti-SARS		*Docking score (kcal/mol)*	*H-bonding*		*Hydrophobic interaction*	
			number	Residues involved	number	Residues involved
GRL-0667	2019-nCoV	-7.0	3	W93, **K105**, **W106**	7	K92, **W106 (2)**, **W106** (3)**, A107
	SARS	-9.3	6	W107, C112, G164, D165*, G272, Y274	5	Y113, L163, Y265, Y274 (2)
GRL-0617	2019-nCoV	-6.6	2	L162, Y264	8	L162, P247, P248, Y264 (2), Y268 (2), T301
	SARS	-8.4	4	L163, D165 (2), Y274	5	D165, P249, Y265, Y269, T302
Mycophenolic Acid	2019-nCoV	-5.7	7	**K105***, **W106 (2)**, H272, H272*, D286, A288	1	L289
	SARS	-8.2	3	G164, G272, Y274	1	Y265

Table 2 The interactions formed between anti-HCV compounds (Telaprevir, Boceprevir, and Grazoprevir) and 2019-nCoV PLpro upon docking. The Star (*) represents salt bridges while the douple stars (**) represents π-π contact.

Anti-HCV		*Docking score (kcal/mol)*	*H-bonding*		*Hydrophobic interaction*	
			number	Residues involved	number	Residues involved
Telaprevir	2019-nCoV	-6.6	8	**W106**, T265, H272, K274, D286 (3), A288	3	**K105**, **W106 (2)**
	HCV	-8.0	10	Q59 (3), H75, K154, G155, S157 (2), A175 (2)	6	I150, L153, K154, F172, A174 (2)
Boceprevir	2019-nCoV	-6.6	4	**W106**, N109 (2), H272	5	**K105**, **W106 (4)**
	HCV	-7.4	10	H75 (2), G155, S157 (3) ,R173, A175 (3)	7	H75 (2), I150, K154 (2), V176, D186
Grazoprevir	2019-nCoV	-6.8	4	**K105**, **W106**, K274, D286	3	**W106**, T265, L289
	HCV	-11.0	10	H75 (2), G155, S156, S157 (3), R173, A175 (2)	13	Q59, F61 (2), H75 (2), H75**, D99, I150, F172, R173, a175, V176, D186

In summary, both anti-SARS PL^{pro} (GRL-0667, GRL-0617, and Mycophenolic acid) and anti-HCV NS3 (Telaprevir, Boceprevir, and Grazoprevir) can bind to the active site (C112, H273, and D287) of 2019-nCoV PL^{pro}. The binding energies for 2019-nCoV PL^{pro} are slightly less than that calculated for SARS PL^{pro} and HCV. On the other hand, at least seven interactions are established between 2019-nCoV PL^{pro} and each tested compound in this study (either H-bonds or hydrophobic interactions) suggesting possible targeting of 2019-nCoV PL^{pro} using anti-SARS and anti-HCV drugs.

Conclusion

Wuhan's novel coronavirus has a significant health concern since the last outbreak of these types of viruses. SARS in the year 2002 to 2003 in China left more than 700 deaths and 8000 cases in hospitals. Middle East region has an entirely different infection pattern of MERS leaving again about 800 deaths

and 2500 hospitalizations. The present study aimed to test and suggest possible inhibitor drugs used against SARS and HCV proteases. Both anti-SARS PL^{pro} (GRL-0667, GRL-0617, and Mycophenolic acid) and anti-HCV NS3 (Telaprevir, Boceprevir, and Grazoprevir) can bind to the active site of 2019-nCoV PL^{pro} and hence, may contradict viral replication.

Declarations

Competing Interest

All the authors declare that there is no competing interest in this work.

Data Availability

The docking structures are available upon request from the corresponding author

References

1 Hui, D. S. *et al.* The continuing 2019-nCoV epidemic threat of novel coronaviruses to global health — The latest 2019 novel coronavirus outbreak in Wuhan, China. *International Journal of Infectious Diseases* **91**, 264-266, doi:10.1016/j.ijid.2020.01.009 (2020).

2 Bogoch, I. I. *et al.* Pneumonia of Unknown Etiology in Wuhan, China: Potential for International Spread Via Commercial Air Travel. *Journal of Travel Medicine*, doi:10.1093/jtm/taaa008 (2020).

3 Organization, W. H. Surveillance case definitions for human infection with novel coronavirus (nCoV): interim guidance v1, January 2020. (World Health Organization, 2020).

4 Organization, W. H. Laboratory testing of human suspected cases of novel coronavirus (nCoV) infection: interim guidance, 10 January 2020. (World Health Organization, 2020).

5 Organization, W. H. Infection prevention and control during health care when novel coronavirus (nCoV) infection is suspected: interim guidance, January 2020. (World Health Organization, 2020).

6 Parr, J. (British Medical Journal Publishing Group, 2020).

7 Yang, L. China confirms human-to-human transmission of coronavirus. (2020).

8 Elfiky, A. A., Mahdy, S. M. & Elshemey, W. M. Quantitative structure-activity relationship and molecular docking revealed a potency of anti-hepatitis C virus drugs against human corona viruses. *Journal of Medical Virology* **89**, 1040-1047, doi:10.1002/jmv.24736 (2017).

9 Chan, J. F. *et al.* Middle East respiratory syndrome coronavirus: another zoonotic betacoronavirus causing SARS-like disease. *Clinical microbiology reviews* **28**, 465-522 (2015).

10 WHO. *Middle East respiratory syndrome coronavirus (MERS-CoV)*, 2016).

11 Hemida, M. G. & Alnaeem, A. Some One Health based control strategies for the Middle East respiratory syndrome coronavirus. *One Health* **8**, 100102, doi:https://doi.org/10.1016/j.onehlt.2019.100102 (2019).

12 Báez-Santos, Y. M., Mielech, A. M., Deng, X., Baker, S. & Mesecar, A. D. Catalytic Function and Substrate Specificity of the Papain-Like Protease Domain of nsp3 from the Middle East Respiratory Syndrome Coronavirus. *Journal of Virology* **88**, 12511-12527, doi:10.1128/jvi.01294-14 (2014).

13 Organization, W. H. Clinical management of severe acute respiratory infection when Middle East respiratory syndrome coronavirus (MERS-CoV) infection is suspected: interim guidance. (World Health Organization, 2019).

14 Elfiky, A. A. & Ismail, A. Molecular dynamics and docking reveal the potency of novel GTP derivatives against RNA dependent RNA polymerase of genotype 4a HCV. *Life Sciences* **238**, 116958, doi:https://doi.org/10.1016/j.lfs.2019.116958 (2019).

15 Elfiky, A. A. Novel Guanosine Derivatives as Anti-HCV NS5b Polymerase: A QSAR and Molecular Docking Study. *Medicinal Chemistry* **15**, 130-137 (2019).

16 Elfiky, A. A. & Ismail, A. M. Molecular Modeling and Docking revealed superiority of IDX-184 as HCV polymerase Inhibitor. *Future Virology* **12**, 339-347 (2017).

17 Elfiky, A. A. & Elshemey, W. M. Molecular dynamics simulation revealed binding of nucleotide inhibitors to ZIKV polymerase over 444 nanoseconds. *Journal of Medical Virology* **90**, 13-18, doi:10.1002/jmv.24934 (2018).

18 Elfiky, A. A. Zika Virus: Novel Guanosine Derivatives revealed strong binding and possible inhibition of the polymerase. *Future Virology* **12**, 721-728 (2017).

19 Berman, H., Henrick, K. & Nakamura, H. Announcing the worldwide Protein Data Bank. *Nat Struct Mol Biol* **10**, 980-980 (2003).

20 Artimo, P. *et al.* ExPASy: SIB bioinformatics resource portal. *Nucleic acids research* **40**, W597-W603 (2012).

21 NCBI. *National Center of Biotechnology Informatics (NCBI) database website http://www.ncbi.nlm.nih.gov/*, <http://www.ncbi.nlm.nih.gov/> (2020).

22 Biasini, M. *et al.* SWISS-MODEL: modelling protein tertiary and quaternary structure using evolutionary information. *Nucleic Acids Research* **42**, W252-W258, doi:10.1093/nar/gku340 (2014).

23 Altschul, S. F. *et al.* Gapped BLAST and PSI-BLAST: a new generation of protein database search programs. *Nucleic acids research* **25**, 3389-3402 (1997).

24 SAVES. Structural Analysis and Verification Server website (2020).

25 Williams, C. J. *et al.* MolProbity: More and better reference data for improved all-atom structure validation. *Protein Science* **27**, 293-315 (2018).

26 Laskowski, R. A., Rullmann, J. A. C., MacArthur, M. W., Kaptein, R. & Thornton, J. M. AQUA and PROCHECK-NMR: Programs for checking the quality of protein structures solved by NMR. *Journal of Biomolecular NMR* **8**, 477-486, doi:10.1007/bf00228148 (1996).

27 Eisenberg, D., Lüthy, R. & Bowie, J. U. in *Methods in enzymology* Vol. 277 396-404 (Elsevier, 1997).

28 Joan Pontius, J. R. a. S. J. W. Deviations from Standard Atomic Volumes as a Quality Measure for Protein Crystal Structures. *Journal of molecular biology* **264**, 121–136 (1996).

29 Hooft, R. W., Vriend, G., Sander, C. & Abola, E. E. Errors in protein structures. *Nature* **381**, 272, doi:10.1038/381272a0 (1996).

30 Summers, K. L., Mahrok, A. K., Dryden, M. D. & Stillman, M. J. Structural properties of metal-free apometallothioneins. *Biochem Biophys Res Commun* **425**, 485-492, doi:10.1016/j.bbrc.2012.07.141 (2012).

31 Elfiky, A. A. The antiviral Sofosbuvir against mucormycosis: an in silico perspective. *Future Virology* **0**, null, doi:10.2217/fvl-2019-0076 (2020).

32 Lii, J. H. & Allinger, N. L. Molecular mechanics. The MM3 force field for hydrocarbons. 3. The van der Waals' potentials and crystal data for aliphatic and aromatic hydrocarbons. *Journal of the American Chemical Society* **111**, 8576-8582, doi:10.1021/ja00205a003 (1989).

33 Trott, O. & Olson, A. J. AutoDock Vina: Improving the speed and accuracy of docking with a new scoring function, efficient optimization, and multithreading. *Journal of Computational Chemistry* **31**, 455-461, doi:10.1002/jcc.21334 (2010).

34 CID=46174170. National Center for Biotechnology Information. PubChem Database. .

35 CID=24941262. National Center for Biotechnology Information. PubChem Database. .

36 CID=446541. National Center for Biotechnology Information. PubChem Database. Mycophenolic acid, .

37 CID=3010818. National Center for Biotechnology Information. PubChem Database. Telaprevir, .

38 CID=10324367. National Center for Biotechnology Information. PubChem Database. Boceprevir,.

39 CID=44603531. National Center for Biotechnology Information. PubChem Database. Grazoprevir, .

40 Salentin, S., Schreiber, S., Haupt, V. J., Adasme, M. F. & Schroeder, M. PLIP: fully automated protein–ligand interaction profiler. *Nucleic acids research* **43**, W443-W447 (2015).

41 Báez-Santos, Y. M., John, S. E. S. & Mesecar, A. D. The SARS-coronavirus papain-like protease: structure, function and inhibition by designed antiviral compounds. *Antiviral research* **115**, 21-38 (2015).

42 Malcolm, B. *et al.* SCH 503034, a mechanism-based inhibitor of hepatitis C virus NS3 protease, suppresses polyprotein maturation and enhances the antiviral activity of alpha interferon in replicon cells. *Antimicrobial agents and chemotherapy* **50**, 1013-1020 (2006).

43 Morris, G. M. *et al.* AutoDock4 and AutoDockTools4: Automated Docking with Selective Receptor Flexibility. *Journal of computational chemistry* **30**, 2785-2791, doi:10.1002/jcc.21256 (2009).

Figures

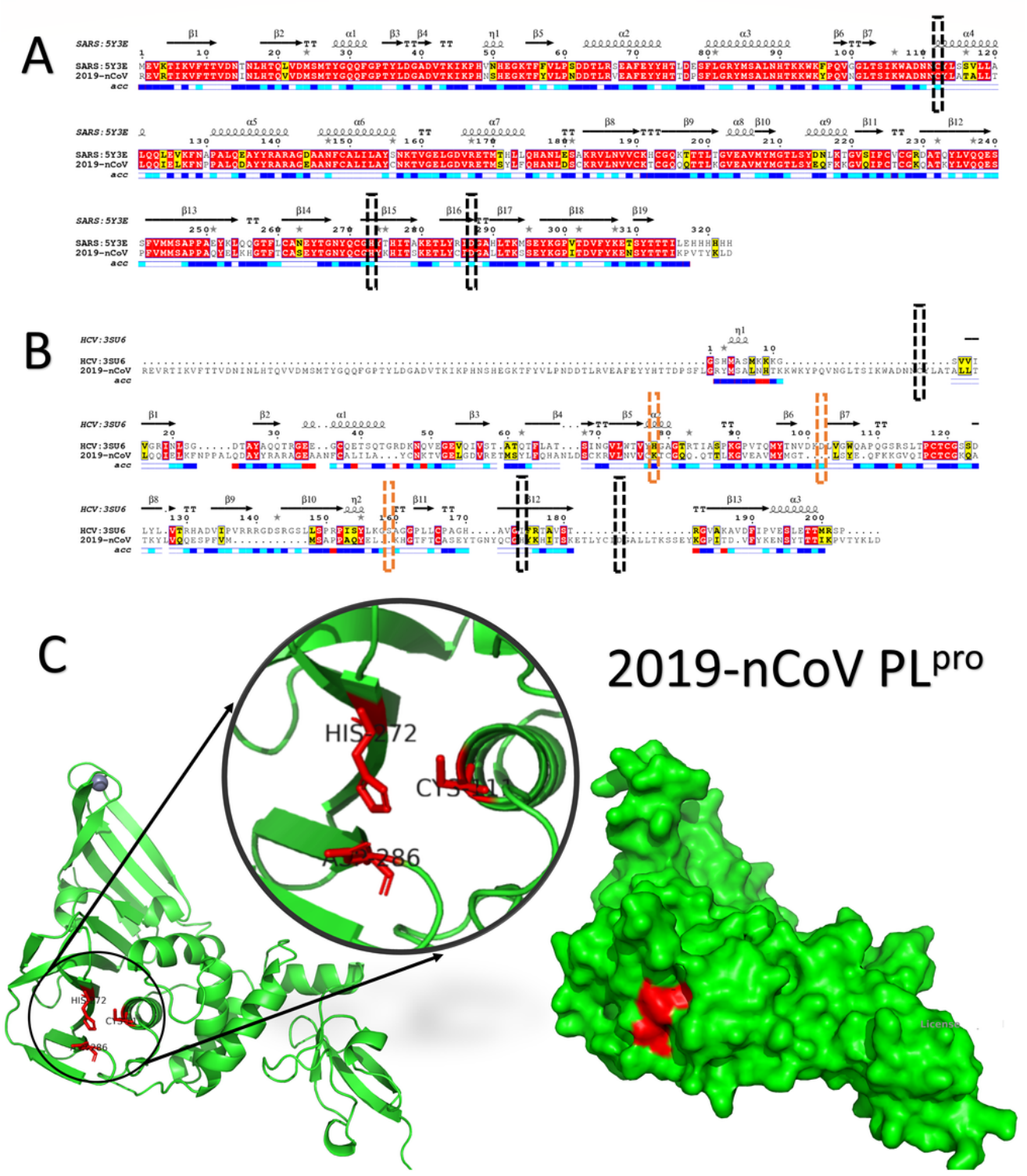

Figure 1

(A) Pairwise sequence alignment of SARS HCoV PLpro (PDB ID: 5Y3E) against the Wuhan 2019-nCoV PLpro. (B) Pairwise sequence alignment of HCV NS3 (PDB ID: 3SU6) against the Wuhan 2019-nCoV PLpro. Red highlights indicate identical residues, while yellow highlights are less conserved. Secondary structures are represented at the top of the alignments, while the surface accessibility is shown at the bottom (blue: highly accessible, cyan: partially accessible, while white is for buried). The black dashed

rectangles mark active sites of both 2019-nCoV PLpro and SARS PLpro (C112, H273, and D287) while orange rectangles mark the active site of HCV NS3 (H78, D102, and S159). The alignment is performed using the CLUSTAL omega web server and represented by ESpript 3. (C) The newly emerged Wuhan 2019-nCoV PLpro model built by Swiss Model in the green cartoon (left) and surface (right) representations. The active site residues are represented in red sticks for clarification (see the enlarged panel).

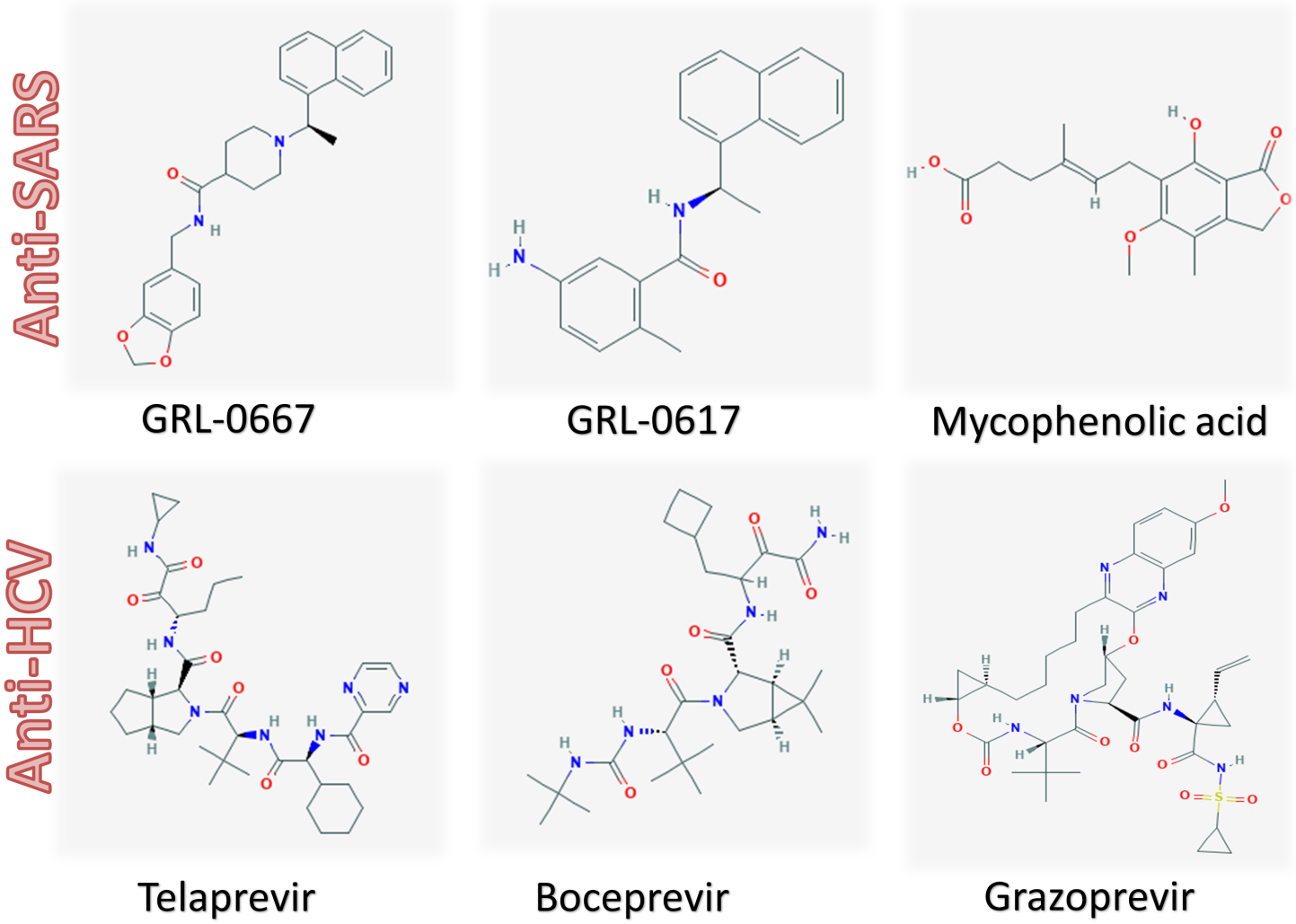

Figure 2

2D structures of the anti-SARS PLpro drugs (top) (GRL-0667, GRL-0617, and Mycophenolic acid) and anti-HCV NS3 drugs (bottom) (Telaprevir, Boceprevir, and Grazoprevir) retrieved from PubChem database. Carbon atoms not explicitly represented by a letter, but with black lines, N stands for Nitrogen, O stands for Oxygen, S stands for Sulfur, and H stands for Hydrogen.

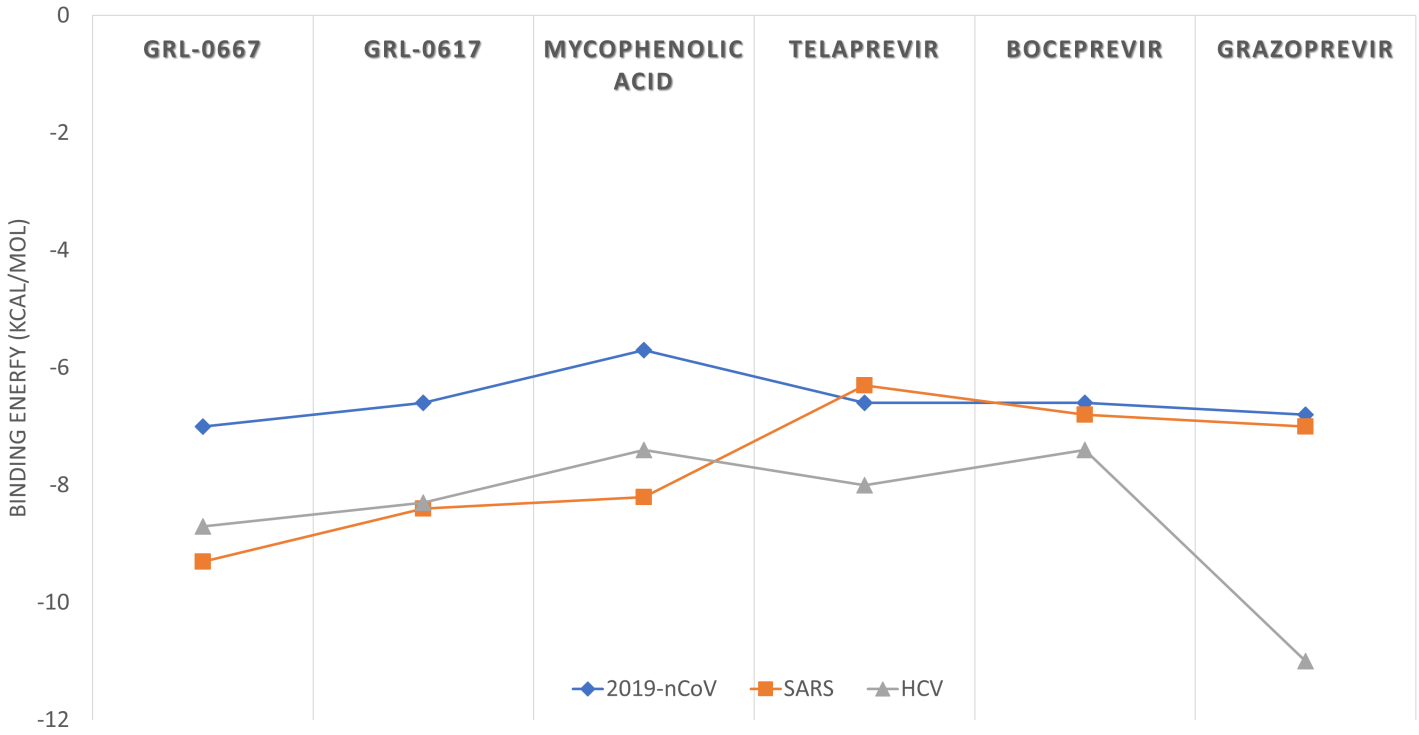

Figure 3

Binding energies calculated by AutoDock Vina for the docking of the anti-SARS PLpro drugs (GRL-0667, GRL-0617, and Mycophenolic acid) and anti-HCV NS3 drugs (Telaprevir, Boceprevir, and Grazoprevir) against 2019-nCoV PLpro (blue line), SARS PLpro (orange line), and HCV NS3 (gray line).

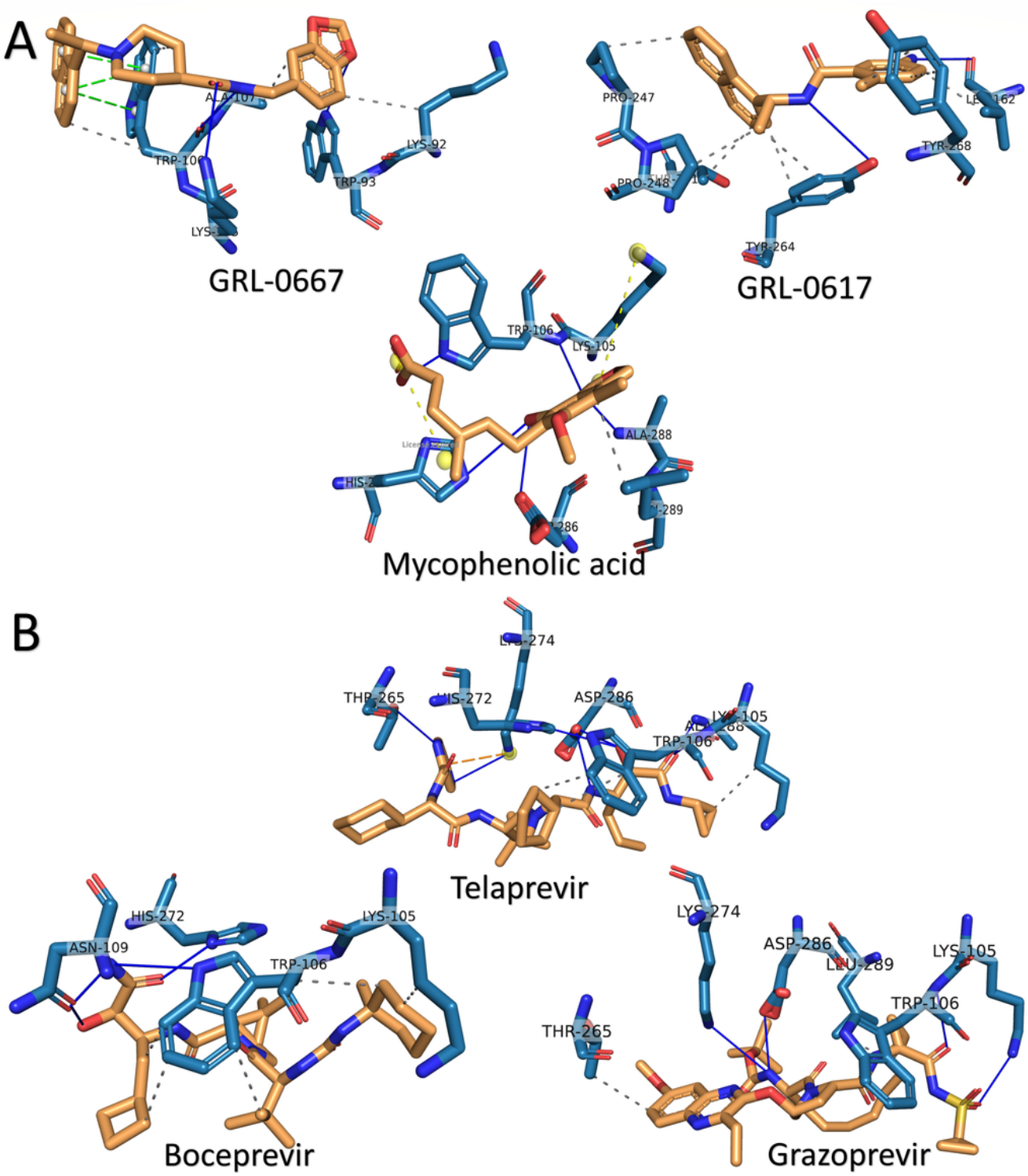

Figure 4

The interaction pattern for 2019-nCoV PLpro against the anti-SARS PLpro (A) and anti-HCV NS3 (B). PyMOL software is used to represent the docking poses using colored sticks. Orange sticks represent the drugs while blue stick for the 2019-nCoV PLpro residues involved in the binding (labeled with its three-letter codes).